Journal of GeoEngineering, Vol. 14, No. 2, pp. 97-107, June 2019
http://dx.doi.org/10.6310/jog.201906_14(2).5

EFFECTS OF WEATHERING ON THE SMALL STRAIN BEHAVIOUR OF DECOMPOSED VOLCANIC ROCKS

Ismail Adeniyi Okewale [1]

ABSTRACT

In this study, the effects of weathering on the stiffness characteristics and small strain behaviour of decomposed volcanic rocks were investigated in detail. Few studies exist on the small strain behaviour of weathered materials and the studies on geomaterials resulting from decomposition of volcanic rocks are very scarce. The study investigated the small strain behaviour of decomposed volcanics in the reconstituted and intact states, allowing for the effect of structure. This was achieved by carrying out extensive triaxial tests using multi-directional bender elements and high resolution linear variable differential transformers on the samples of various degrees of weathering from different locations, depths and formations. Elastic model parameters obtained from experimental data are used as stiffness parameters and they are related with engineering indices and depth which is very important from geological point of view. The effect of heterogeneity is much more obvious at small strain. The effect of structure is generally small using bender elements at small strain. Weathering affects the stiffness of decomposed volcanic rocks and more effect is seen particularly for the reconstituted samples. Plasticity and fines content might be controlling parameters for the stiffness of decomposed volcanics.

Key words: Weathering, stiffness, structure, bender elements, volcanic saprolites.

1. INTRODUCTION

Predicting the deformation around geotechnical structures subjected to loading is very important in engineering design and analysis. In order to achieve the prediction more accurately, the small strain behaviour of the geomaterials around the structure must be correctly defined. Also, the stiffness characteristics play an important role in predicting the soil-structure interaction as well as in earthquake engineering. Extensive studies have been conducted on the small strain behaviour of clays and sands (*e.g.,* Cuccovillo and Coop 1997; Gasparre and Coop 2006; Gasparre *et al.* 2007; Gasparre *et al.* 2014; Pennington *et al.* 1997). However, the studies on small strain behaviour of weathered geomaterials are still limited compared to clays and sands. Weathered rocks are abundant in tropical and subtropical areas of the world and in Hong Kong particularly, weathered geomaterials are widespread and many geotechnical structures are built in and on them. Also, in many areas where these geomaterials are found they are used as fill materials for engineering projects. While few studies are available for the granitic rocks (*e.g.,* Ng *et al.* 2000; Ng *et al.* 2004; Ng and Wang 2001; Viana Da Fonseca *et al.* 1997), investigations into the small strain behaviour of weathered volcanic rocks are very limited.

This paper presents the effects of weathering on the stiffness characteristics and small strain behaviour of Highly Decomposed Volcanic rocks (HDV) and Completely Decomposed Volcanic rocks (CDV) with various weathering degrees from different locations, formations and depths of occurrence in the intact and reconstituted states. This work is however different from Okewale and Coop (2017) which presented the mechanics of behaviour of decomposed volcanic rocks linking geological structures with geotechnical parameters, Okewale and Coop (2018) that reported different approaches (physical, mineralogical and chemical indices) to predict and analyse the behaviour (in-situ, compression and shearing) of decomposed volcanic rocks and Okewale (2019) which investigated influence of fines on the compression behaviour of decomposed volcanics. This was achieved by carrying out triaxial tests using different apparatuses and combining bender elements and local instrumentations in isotropic compression and shearing. This work is unique because there are hardly any studies that have systematically investigated the effects of weathering on the stiffness of weathered geomaterials and almost non-existent for the decomposed volcanic rocks. The approach is also novel in how the elastic model parameters are related to geological processes of weathering and engineering indices useful to practising engineers.

2. MATERIALS AND METHODS

The samples used for the laboratory tests were decomposed volcanic rocks, locally called tuffs. The samples belong to three different formations namely: Ap Lei Chau (AlC, fine-grained tuffs), Mount Davis (MtD, coarse-grained tuffs) and Tai Mo Shan (TMS, coarse-grained tuffs). Formations are used for volcanic rocks due to their complexity. The block and mazier (tube) samples were taken from different locations in Hong Kong under the supervision of Geotechnical Engineering Office (GEO) of Hong Kong as given in Fig. 1. Block samples were taken from shallow trial pits (0.7 ~ 3.5 m) and the mazier samples were from relatively deeper depths (1 ~ 14 m). Based on international standards (six grade classification), the samples corresponded to grade IV (highly decomposed) and grade V (completely decomposed) rocks (ISRM 2007; Irfan 1996). According to GEO (1988) classification system for Hong Kong geomaterials, a de-

Manuscript received November 7, 2018; revised January 18, 2019; accepted March 23, 2019.
[1] Lecturer (corresponding author), Department of Mining Engineering, Federal University of Technology Akure, P.M.B. 704, Ondo State, Nigeria (e-mail: iaokewale@futa.edu.ng).

scription of consistency of sample were added and these are extremely weak (ew), extremely weak to very weak (ewvw), very weak (vw), very weak to weak (vww), weak (w) and weak to moderately weak (wmw). For simplicity, the samples are represented by acronyms based on the degrees of weathering for the CDV and HDV. In the acronyms, the letters represent the weathering degree followed by the number which stands for the consistency. For the CDV, 5 is used for the ew, 4 for the ewvw, 3 for the vw, 2 for the w and 1 for the wmw. Also, 2 is used for the vww and 1 for the wmw in the HDV samples. These descriptions of consistency, although subjective were made at the time of sampling by experienced geologists or engineers on site. However, the descriptions were verified by the author in the laboratory using visual inspection and slaking method (soaking the samples in water). The details of sample description are given in Table 1.

The reconstituted samples were prepared by adding distilled water to make slurries. Reconstituted samples are those in which the natural cohesion (bonding) has been removed, that is the samples have been completely destructured. Reconstituted samples are needed to assess the aspects of small strain behaviour resulting solely from constituent particles and those that relate to the structure (bonding and fabric). Structure of weathered geomaterials is the physical and chemical equilibrium between the particles that develops during geological processes of weathering. The effects of structure (degree of enhanced stiffness) are assessed by comparing the behaviour of samples in the intact state to its reconstituted state. The fundamental effect of structure is increase in stiffness as a result of bonding and fabric. The samples were prepared directly on the platen for 50 mm diameter samples using a carefully designed mould.

The intact samples were prepared by cutting the tube containing the sample carefully to the required length using diamond tipped rotary saw. A machine end cutter was then used to cut several slots carefully with the sample firmly supported. The segments of the tube were peeled off. The sample and the perimeter of the samples well dressed. This method of retrieving the sample prevents disturbance of the sample compared to extrusion method.

Table 1 Details of the sample descriptions

Location/ weathering degree	Sample type/ borehole	Formation	Acronym	Depth (m)	Grading
A/ewCDV	Block	AlC	CDV-5	0.7 ~ 1	Fine
B/ewCDV	Block	AlC	CDV-5	1.7 ~ 2	Fine
C/ewCDV	Block	AlC	CDV-5	2.4 ~ 3.5	Fine
D/wmwHDV	Block	AlC	HDV-1	0.7 ~ 1	Fine
E/vwwHDV	Block	AlC	HDV-2	1.5 ~ 2.6	Fine
H/wmwCDV	Mazier (DH1)	AlC	CDV-1	1 ~ 1.4	Fine
I/ewCDV	Mazier (DH1)	AlC	CDV-5	3.6 ~ 4.6	Fine
J/ewCDV	Mazier (DH1)	AlC	CDV-5	4.7 ~ 5.7	Fine
K/vwCDV	Mazier (DH2)	AlC	CDV-3	4.5 ~ 5.5	Fine
L/ewCDV	Mazier (DH1)	TMS	CDV-5	4 ~ 5	Coarse
M/ewCDV	Mazier (DH2)	TMS	CDV-5	10.7 ~ 11.7	Coarse
N/ewCDV	Mazier (DH4)	MtD	CDV-5	5.86 ~ 6.31	Coarse
O/ewvwCDV	Mazier (DH2)	AlC	CDV-4	8.10 ~ 8.35	Fine
P/wCDV	Mazier (DH5)	AlC	CDV-2	13.3 ~ 13.95	Fine

Note: AlC: Ap Lei Chau formation, TMS: Tai Mo Shan formation, MtD: Mount Davis formation; ew: extremely weak, ewvw: extremely weak to very weak, vw: very weak, w: weak, vww: very weak to weak, wmw: weak to medium weak; CDV: Completely Decomposed Volcanic rocks, HDV: Highly Decomposed Volcanic rocks.

Three computer controlled triaxial apparatuses, namely, Imperial College (IC) stress path cell, GDS stress path cell and GDS modified hollow cylinder triaxial were used for the tests. The IC has cell capacity of 800 kPa and was used for all the reconstituted samples. Both GDS stress path and hollow cylinder have cell capacity of 2 MPa and they were used for the intact samples. The IC cell was equipped with vertical and lateral bender elements (Pennington *et al.* 1997; Clayton *et al.* 2004) as well as miniature submersible linearly variable differential transformers (LVDTs) which measure local axial and radial strains (Cuccovillo and Coop 1997). Bender Elements (BE) are powerful transducers made from piezoelectric ceramic bimorphs and used to determine shear wave velocity and consequently, the small strain shear modulus of geomaterials.

The whole system of the apparatus was flushed to ensure that no air is trapped in the cell, back and pore pressure lines. For the coarser and finer grained reconstituted samples, a de-aired porous stone was placed on the pedestal and a membrane placed around it and sealed with O-rings. A two-part split mould was put in place and the membrane stretched around it and held against the mould by applying a suction. The mould was then filled with sample and top platen was then placed on top and membrane rolled around it and sealed with O-rings. A small suction was applied by attaching a burette placed below the level of apparatus to the drainage and the mould was removed after the volume in the burette had stabilised. The dimensions of the samples were then taken allowing for the thickness of membrane.

The intact samples held in the cradle were placed on porous stone on the pedestal without any support. A membrane was put around the sample with the aid of membrane stretcher and then sealed at the base and top by O-rings after putting the top platen in place. After taken the initial measurements, the triaxial chamber was put in place, tightened by tie rods and filled with water. A cell pressure of 20 ~ 30 kPa was applied for the reconstituted samples or a cell pressure equal to the total in-situ effective stress for the intact samples. Back pressure saturation was used and B values between 0.95 and 1 were achieved for all the tests conducted. The saturation was slow due to low permeability and much slower for the intact samples, usually for several days.

An isotropic compression stage was followed by the shearing of the samples. The volume change in isotropic compression and shearing was measured by local transducers and an external volume gauge transducer connected to back pressure line. After shearing, the cell was drained and the sample carefully recovered without disturbance. The final measurements of dimensions were taken and the sample oven-dried for final water content.

Three pairs of bender elements (vertical and lateral) were used to measure shear wave in three different planes in the samples. A pair of bender elements was inserted at the top and bottom ends of the samples and two pairs were inserted at the mid-height of the samples opposite to each other. The vertical and lateral bender elements allow the three pairs of shear waves ($v_{s(vh)}$, $v_{s(hv)}$, and $v_{s(hh)}$) travelling through the samples to be measured. The associated shear moduli (G_{vh}, G_{hv}, and G_{hh}) were subsequently calculated. The subscripts *vh*, *hv*, and *hh* are the directions (horizontal and vertical) of propagation and polarisation of shear waves, respectively.

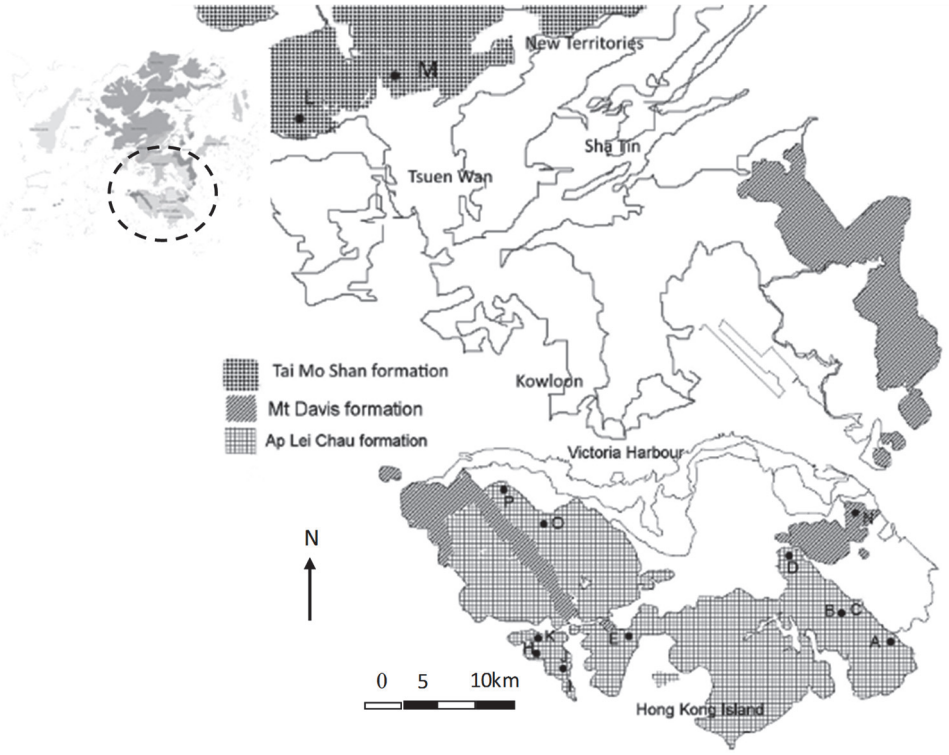

Fig. 1 Map of sample locations (after Okewale and Coop 2018)

The GDS stress path cell was equipped with vertical bender element, axial LVDTs and a radial strain belt which also has an LVDT. The arrangements of bender elements and axial LVDTs were similar to the IC cells. The radial strain belt was attached at the mid-height of the samples. The GDS hollow cylinder was equipped with only axial and radial LVDTs. The positioning of the LVDTs was similar to those in the IC cells. The samples were loaded isotropically in a continuous manner and the bender element measurements were taken during the stages. Bender element was excited with a single shot sine wave having a wide range of frequencies and both the input and the output were measured and recorded by an oscilloscope.

The first arrival time method was used to calculate the shear wave velocity of the samples. Once the arrival time (t_a) was identified, the velocity (v_s) of the travelling wave was estimated based on tip to tip distance of the bender elements. The shear modulus (G) values were calculated from the velocity of travelling wave (v_s) through the sample as follows:

$$G = \rho v_s^2 \tag{1}$$

where ρ is the bulk density of the sample.

The local instrumentations (strain gauges) were used to measure axial and radial displacements which were used in the calculation of shear modulus in the small strain region typically shear strain less than 0.1% during shearing probes.

The void ratios, ($e = v - 1$), of the samples were estimated from specific volumes (v). The initial specific volumes were derived from the initial dimensions, weight and water content, while the final v was derived from final water content and final dimensions, back-calculating the initial value using the measured volumetric strain. Several methods were used to make the measurements but they were made to be as independent as possible in order to improve the confidence.

3. RESULTS AND DISCUSSIONS

3.1 Index and Mechanical Properties

Figure 2 presents the particle size distribution curves for all the samples as determined from wet sieving and sedimentation techniques. The samples are generally classified as HDV and CDV and further sub-divided into different weathering descriptions (Fig. 2). Solid lines are used for the HDV and broken lines for the CDV and a decrease in line weights and lighter colours of symbols correspond to an increase in the degrees of weathering. The broken lines and symbols are used for the TMS formation. Based on British Standard, demarcations are put at 0.002 and 0.063 mm to divide the samples into clay, silt and sand fractions.

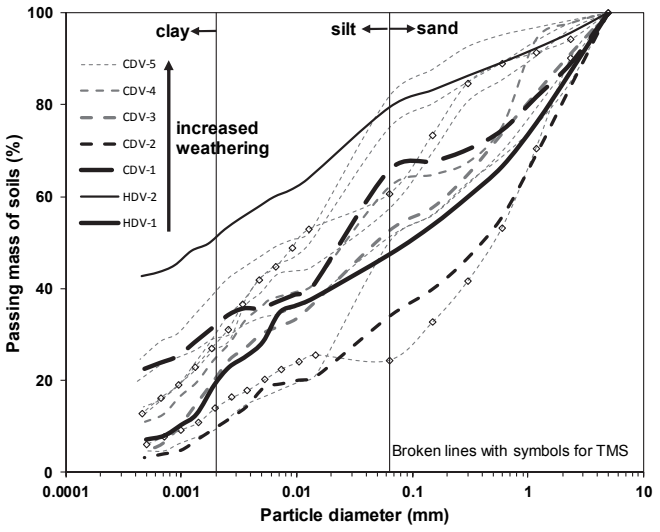

Fig. 2 Grading curves for the samples (modified from Okewale and Coop 2018)

The samples are all well graded and can be classified as silty sand. The clay fraction (CF) ranges from 10% to 52%. The liquid limit (LL) and plastic limit (PL) were determined through Atterberg Limit tests (BS 1377:2 1990). The plasticity indices (PI) range from 9.2% to 34.7%. The details of the index properties are given in Table 2.

The details of basic mechanical properties are given in Table 3. The heterogeneous nature of the samples is responsible for the scattered data of the mechanical properties. The density (ρ) seems increasing with depth and in-situ specific volume (v) tends to increase with weathering. The strength parameter (M) reduces with weathering and the trend of tangent Young's modulus (E_t) with weathering is not clear.

3.2 Small Strain Behaviour in Isotropic Compression

Elastic shear modulus (G_o) was determined for samples of different degrees of weathering subjected to isotropic compression at different mean effective stresses (p') levels using bender elements. Twenty six tests were conducted and the details of the tests are given in Table 4; the tests indicate the location with the first letter, followed by mean effective stress p' at the end of consolidation and then R stands for reconstituted or I for intact samples. Figure 3 presents the elastic shear modulus (G_{vh}) data obtained from vertical bender elements measurements for the reconstituted and intact samples. There is a clear trend of increase in elastic shear modulus with mean effective stress for the reconstituted samples of various weathering degrees, similar to other geomaterials for example granitic saprolite (Jovicic and Coop 1997), clay (Vaggiani and Atkinson 1995), Dogs Bay and Ham River sands (Jovicic and Coop 1997).

Table 2 Details of the index properties of the samples

Location/Acronym	Formation	Depth (m)	LL (%)	PL (%)	PI (%)	CF (%)
A/CDV-5	AlC	0.7 ~ 1	82.8	48.1	34.7	40
B/CDV-5	AlC	1.7 ~ 2	71.7	48.7	23	30
C/CDV-5	AlC	2.4 ~ 3.5	71.3	52.2	19.1	30
J/CDV-5 L/CDV-5	AlC TMS	4.7 ~ 5.7 4 ~ 5	41 35.5	27.8 26.1	13.2 9.4	32 34
M/CDV-5	TMS	10.7 ~ 11.7	–	–	–	17
N/CDV-5	MtD	5.86 ~ 6.31	36	26.1	9.9	10
O/CDV-4	AlC	8.1 ~ 8.35	38.8	25.9	12.9	26
K/CDV-3	AlC	4.5 ~ 5.5	30.4	20.5	9.9	22
P/CDV-2	AlC	13.3 ~ 13.95	31.2	22	9.2	10
H/CDV-1	AlC	1 ~ 1.4	46	25.4	20.6	32
E/HDV-2	AlC	1.5 ~ 2.6	70.7	38.1	32.6	24
D/HDV-1	AlC	0.7 ~ 1	43.3	33.1	10.2	52

Note: LL liquid limit, PL Plastic limit, PI Plasticity index, CF Clay fraction.

Table 3 Details of mechanical properties

Sample	ρ (g/cm^3)	v	M	E_t (MPa)
A/CDV-5	1.60	2.27	1.25	100
B/CDV-5	1.55	1.92	1.43	–
C/CDV-5	1.42	2.07	1.49	–
J/CDV-5 L/CDV-5	1.89 1.70	2.09 1.93	1.35 1.35	240 –
M/CDV-5	1.91	1.64	1.46	700
N/CDV-5	2.02	1.88	1.49	–
O/CDV-4	1.94	1.70	1.5	50
K/CDV-3	1.57	1.95	1.51	520
P/CDV-2	2.19	1.49	1.6	200
H/CDV-1	1.95	1.72	1.5	300
E/HDV-2	1.45	1.89	1.34	–
D/HDV-1	1.35	2.05	1.62	–

Note: ρ Bulk density, v In-situ specific volume, M Strength parameter, E_t Tangent Young's modulus.

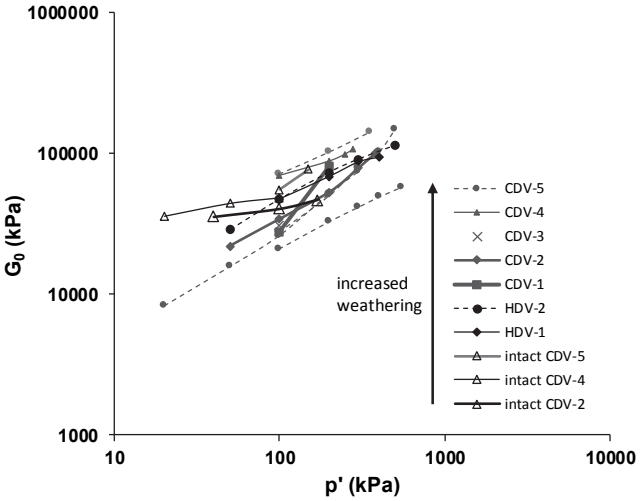

Fig. 3 Elastic shear modulus for the reconstituted and intact samples

Table 4 Details of the tests

Sample	Test	Size (H/D)(mm)	p_c' (kPa)	Shearing condition
A/CDV-5	A500R A50I	100/50 100/50	500 50	CD CU
B/CDV-5	B400R B550R	100/50 100/50	400 550	CD CD
C/CDV-5	C300R	100/50	300	CU
J/CDV-5	J200R (1) J200R (2) J200I (1) J200I (2)	100/50 100/50 150/75 150/75	200 200 200 200	CD CD CU CD
L/CDV-5	L220R	100/50	220	CD
M/CDV-5	M150I	150/75	150	CU
N/CDV-5	N350R	100/50	350	CD
O/CDV-4	O280R O100I	100/50 150/75	280 100	CD CD
K/CDV-3	K100R K400I	100/50 150/75	100 400	CD CU
P/CDV-2	P200R P380R P170I P800I	100/50 100/50 150/75 150/75	200 380 170 800	CD CU CD CU
H/CDV-1	H200R H50I H1000I	100/50 150/75 150/75	200 50 1000	CD CD CD
E/HDV-2	E500R	100/50	500	CD
D/HDV-1	D400R D380R	100/50 100/50	400 380	CD CD

Note: I Intact, R Reconstituted, H Height, D Diameter, p_c' p' at the end of consolidation, CD Consolidated Drained, CU Consolidated Undrained.

The most weathered samples plot below which indicates low stiffness but there seems no clear trend of elastic shear modulus with degree of weathering due to heterogeneity. Similar to other intact geomaterials, for example granitic saprolite (Ng and Wang 2001) and weathered tuff (Ng and Leung 2007), there is no clear increase of elastic shear modulus with mean effective stress for the intact samples. Comparing the intact and reconstituted samples of the same weathering degree from the same location, the moduli of the intact samples are slightly higher than those of the reconstituted samples, indicating small effect of structure. Also, the moduli of the intact samples are not increasing with p', showing the effect of structure.

In order to make comparison between the intact and reconstituted samples as well as samples of different weathering degrees, elastic shear modulus data were normalized to account for the possible effect of void ratios. Different void ratio functions were considered for normalisation; $f(e) = (2.17 - e)^2/(1 + e)$ (Hardin and Richart 1963), $f(e) = (2.97 - e)^2/(1 + e)$ (Hardin and Drnevich 1972), $f(e) = e^{-1.3}$ (Jamiolowski *et al.* 1995; Lo Presti 1995), $f(e) = e^{-2.2}(2.73 + e)/(1 + e)$ (Ng and Leung 2007), $f(e) = (1 + e)^{-2.4}$ (Shibuya *et al.* 1997), but for clarity only $f(e) = e^{-1.3}$ suggested by Jamiolkowski *et al.* (1995) is presented in Fig. 4. These normalizations were also applied to data from shearing probe that will be discussed later.

Figure 4 presents the normalized elastic shear modulus for various weathering degrees. Within the scattered data, the least weathered samples are stiffer, plotting above the most weathered samples for the reconstituted samples. The shear modulus value and the trend with mean effective stress is similar to the values obtained for the Hong Kong HDG/CDG studied by Rocchi and Coop (2015). Generally, trends similar to Fig. 3 are seen even after void ratio normalization is applied.

3.3 Small Strain Behaviour in Shearing

The shear modulus data obtained from shearing probe for the reconstituted samples are presented in Fig. 5. Figure 5(a) presents the stiffness degradation curves for some samples from different locations and various degrees of weathering. Tangent shear modulus ($G_{tan} = \delta q/\delta\varepsilon_s$, where q is deviatoric stress and ε_s is shear strain) is presented in this paper. The least squares regression functions (LINEST), available in Microsoft Excel was used to calculate the moduli. The mean effective stress at the beginning of shearing for each test is indicated in the plots. Empty symbols are used for the CDV and filled symbols for the HDV. Also, same symbol is used for the same weathering degree and the deeper colour indicates the reduction in the degree of weathering. The least weathered samples plot above the most weathered samples indicating that they are stiffer but as a result of heterogeneity which is an important characteristic of weathering processes, the trend with weathering degree is not too clear. The curves degrade fast and show a highly non-linear behaviour similar to what has been found for other reconstituted materials (*e.g.,* granitic saprolite, Dogs Bay sand studied by Jovicic and Coop 1997).

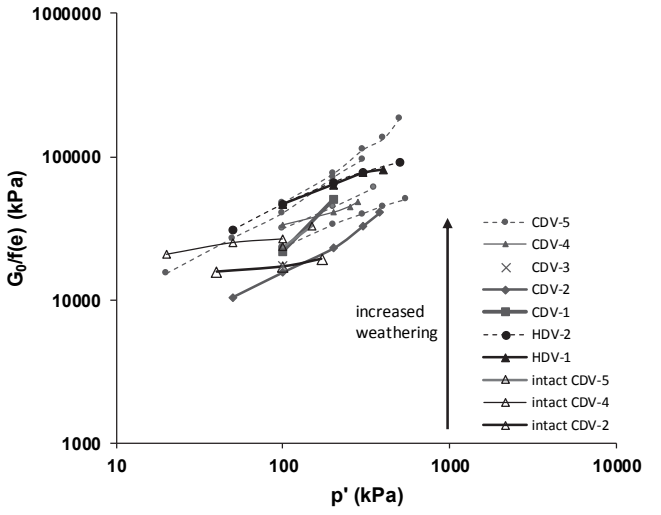

Fig. 4 Normalized elastic shear modulus for the reconstituted and intact samples

Figure 5(b) shows the variation of normalized tangent shear modulus ($G/f(e)$) with shear strain for the reconstituted samples. The same void ratio function used in bender elements probe as discussed earlier is also applied in shearing probe. After removing the possible effect of void ratio, the trend similar to those found for the tangent shear modulus (Fig. 5(a)) is seen.

Figure 6 presents the variation of tangent shear modulus with shear strain for the intact samples. For clarity, only few representative samples are shown and again. Open symbols are used for the CDV and there is no test carried out for the HDV due to collapse nature of the samples during trimming of the block samples. The mean effective stresses at the beginning of the tests are small compared to those of the reconstituted samples because samples were sheared at the estimated in-situ mean effective stress. The behaviour is highly non-linear and the curves degrade fast similar to what has been found for other geomaterials (Ng *et al.* 2000; Wang and Ng 2005). The least weathered sample is stiffer causing the higher position of the curves. The stiffness plots do not give any particular pattern with the degree of weathering and this has also been found for the CDG/HDG studied by Rocchi and Coop (2015). On normalizing the shear stiffness data for the likely effect of void ratio, same trend can still be seen for different weathering degrees (Fig. 6(b)).

The comparisons between normalized tangent shear modulus and the mean effective stress at different strain levels for the reconstituted and intact samples is presented in Fig. 7. In order to overcome the scattered data, a smooth curve was drawn on the decay curves and the approximated values at shear strains of 0.001%, 0.01%, and 0.1% are plotted. A cloud of data is formed at different strain levels (Figs. 7(a) to 7(c)). There seems to be a correlation between the modulus measured and the degree of weathering for the reconstituted samples. The least weathered samples are stiffer, plot above the most weathered samples. For the intact samples, the variations with degrees of weathering do not follow a particular pattern due to the nature of the samples. The data points may form a linear relationship with p', represented by a regression line.

Comparing the variation of shear modulus with mean effective stress at different strain levels for the intact and reconstituted samples allows the effect of structure to be determined. The changing effects of structure on the mechanics is directly related to the geological processes of weathering. Weathering causes disintegration of rocks, thereby weakens and softens the resulting materials and consequently affects both structure and intrinsic behaviour. The major advantage of the effect of structure is that it shows the contribution of bonding and fabric to the mechanical behaviour (stiffness) of the sample. Empty black symbols are used for the intact samples while empty grey and filled symbols

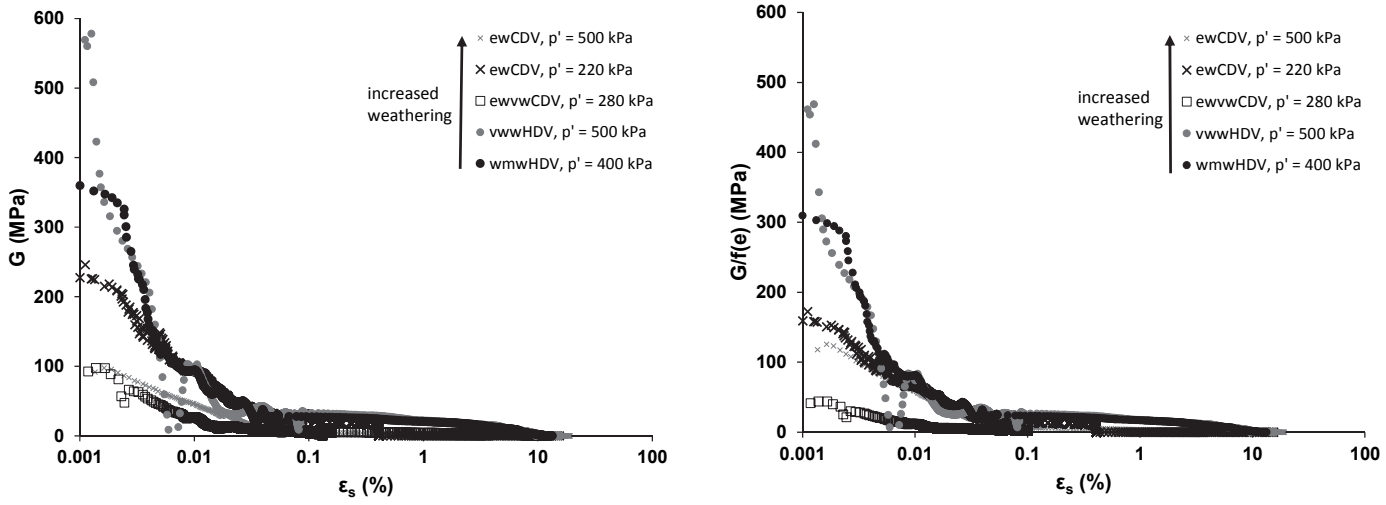

(a) Shear modulus (b) Normalized shear modulus

Fig. 5 Shear and normalized shear stiffness for the reconstituted samples

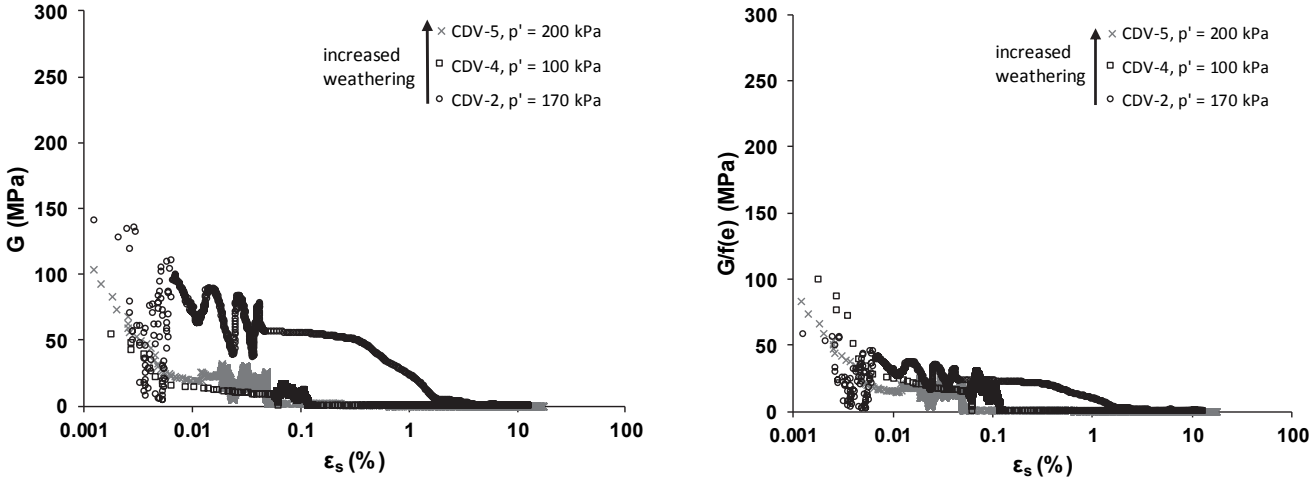

(a) Shear modulus (b) Normalized shear modulus

Fig. 6 Shear and normalized shear modulus for the intact samples

are used for the reconstituted samples. The black and grey broken regression lines represent the trends for the intact and reconstituted samples respectively. At any given strain and based on the regression lines, the moduli of the intact samples are higher than those of the reconstituted samples.

These data are used to construct the lines for the material elastic model parameters (A and n) obtained from experimental data which will be discussed later. The offset between the regression lines of the intact and reconstituted samples may be considered as the degree of enhanced stiffness. The effect of structure is reducing with strain as expected because at critical state, the lines will be coincident as the intact structure would have been erased.

An empirical power function relates shear stiffness G with mean effective stress p', which has been used for clays, sand and other geomaterials (Ng and Wang 2001; Jovicic and Coop 1997; Wroth and Houlsby 1995).

$$\frac{G}{p_r} = A\left(\frac{p'}{p_r}\right)^n \tag{2}$$

where p_r is the reference pressure taken as 1 kPa to make the parameters A and n dimensionless.

Equation (2) above is used to refer to elastic stiffness so that A and n can be used as material parameters. Jovicic and Coop (1997) stated that this same equation can be used for tangent stiffness at large strain, but in this way, A and n will be changing with strain and stress path. In this paper, the same equation is also used for tangent stiffness at small strains calculated during shearing probe and will be discussed later. Generally, samples with higher stiffness will have higher A values and smaller n values. Figure 8 presents the variations of elastic parameters A and n with strain levels. Both parameters obtained using vertical bender elements and those obtained during shear probes are given in the plots. The parameters obtained from the bender elements test are represented by symbols plotted arbitrarily at ε_s = 0.001% while those obtained during shear probes are represented by black and grey lines for the intact and reconstituted samples respectively. Both intact and reconstituted samples are shown for the purpose of comparison.

For the bender elements probes, the A values of the intact samples are greater than those of the reconstituted samples (Fig. 8(a)) and also, the n values of the intact samples are lower than those of the reconstituted samples (Fig. 8(b)). Apart from the little scatter, in the shearing probes, A values reduce and n values

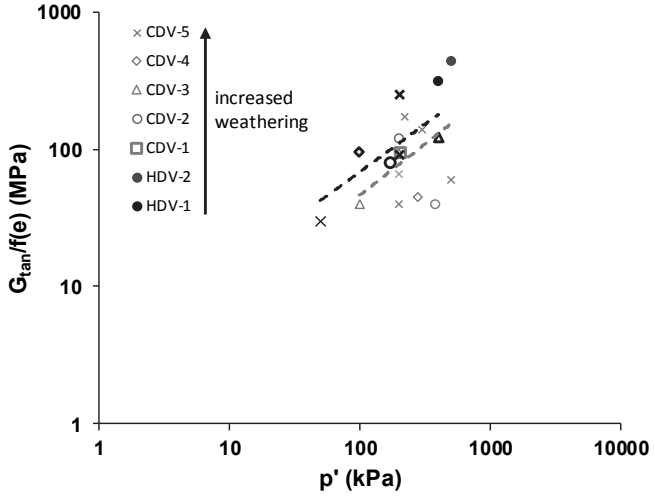

(a) Strain level = 0.001%

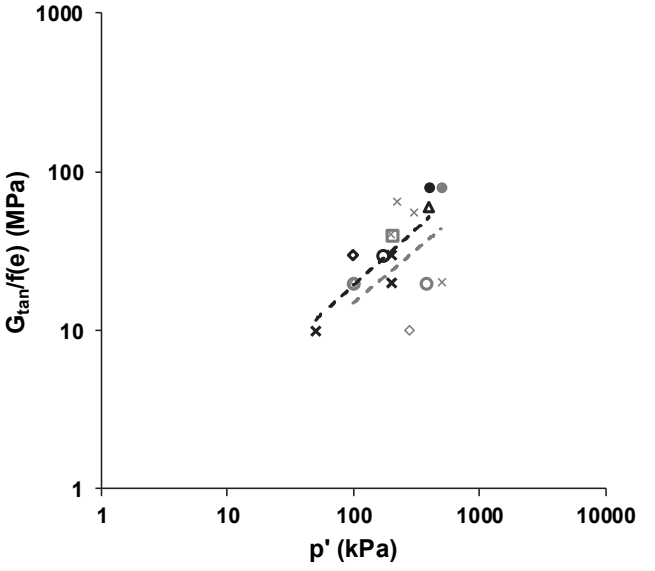

(b) Strain level = 0.01%

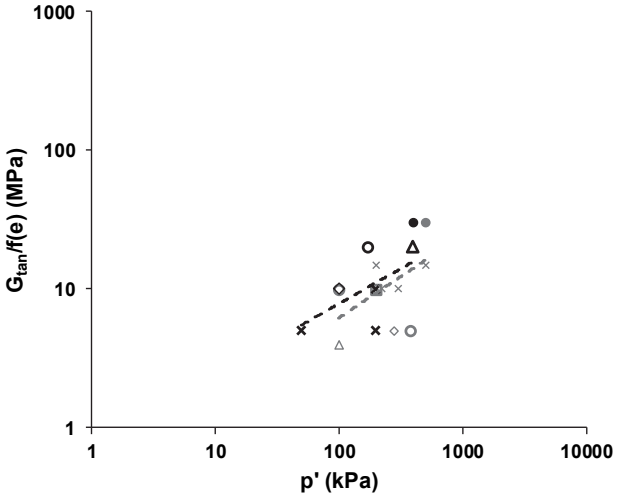

(c) Strain level = 0.1%

Note: Empty black symbols and are for the intact samples; Empty grey, filled symbols and line are for the re constituted samples

Fig. 7 Comparison of the change in normalized shear modulus for the reconstituted and intact samples at different strain levels

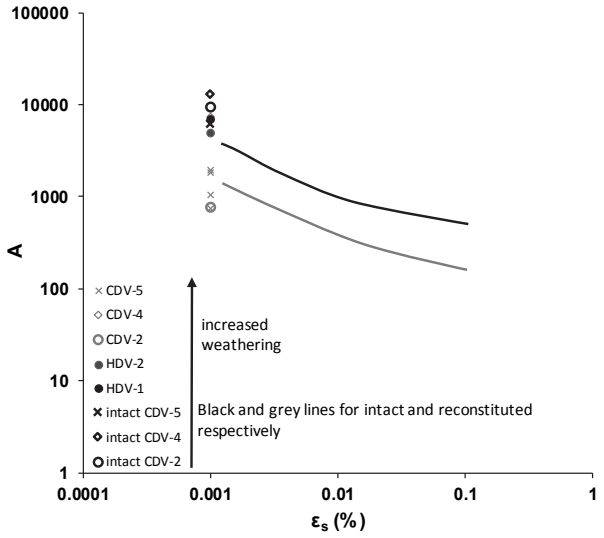

(a) Variation of A

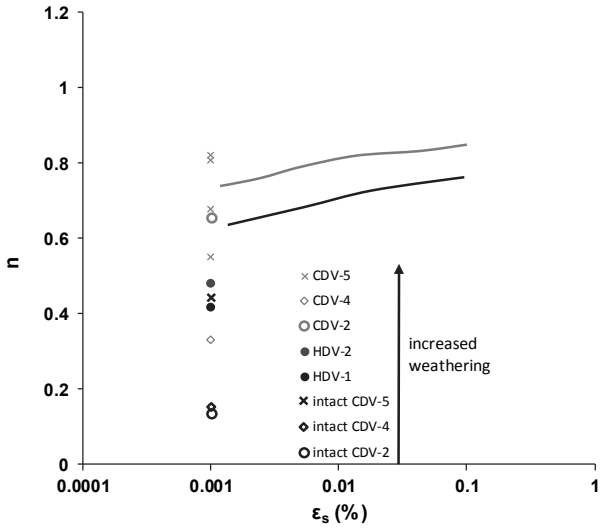

(b) Variation of n

Note: Symbols are the parameters from BE; Black and grey lines for intact and reconstituted respectively

Fig. 8 Variation of parameters with strain

increase with strains for the intact and reconstituted samples. This is similar to what has been found by other researchers (*e.g.,* Jovicic and Coop (1997) for their study on sands).

The parameter A is reducing as expected because at the critical state, the parameters will be zero. The A values for the intact samples are greater than those of the reconstituted samples and also, the n values of the intact samples are less. Although, there is some scatter in the data which may be as a result of heterogeneity, the effect of weathering can be seen for the reconstituted samples. For the A values, the least weathered samples plot above, while for the n values, the least weathered samples plot below, showing that weathering processes reduce the stiffness of the samples.

Comparisons are made between the data obtained in this study and those found in literature for other geomaterials such as London clay (Vaggiani and Atkinson 1995), sands (Jovicic and Coop 1997) and granitic saprolite (Viana Da Fonseca *et al.* 1997; Ng and Wang 2001) and the details are given in Table 5. As stated earlier, the data for the reconstituted samples varies based on the degrees of weathering, but the average value of parameters

Table 5 Comparison of the material parameters for different geomaterials

Sample	*A*	*n*	Author(s)
London clay (R)	1964	0.653	Vaggiani and Atkinson (1995)
Decomposed granite from Seoul (R)	763	0.884	Jovicic and Coop (1997)
Dogs Bay sand (R)	3096	0.686	Jovicic and Coop (1997)
Ham River sand (R)	3899	0.593	Jovicic and Coop (1997)
Granitic saprolite from Portugal (I)	1482	0.819	Viana Da Fonseca *et al.* (1997)
Granitic saprolite from Hong Kong (I)	2535	0.691	Ng and Wang (2001)
CDV (R)	3284	0.562	This study
HDV (R)	5893	0.449	This study
CDV (I)	7516	0.389	This study

NB I intact, R reconstituted

for the CDV (A = 3284, n = 0.562) are within the range found for the other reconstituted geomaterials but the reconstituted HDV has relatively higher A (= 5893) and lower n (= 0.449). The intact samples in this study have larger average value of A (= 7516) and lower average value of n (= 0.389) compared with intact granitic saprolites by Viana Da Fonseca *et al.* (1997) and Ng and Wang (2001).

3.4 Variation of Material Parameters with Engineering Indices and Weathering

An attempt is made to relate the material parameters with plasticity and grading descriptors (*e.g.*, fines content) to capture the relationship between the stiffness and physical indices. This will show how weathering processes affect the engineering descriptors as well as how it relates to stiffness characteristics of decomposed volcanics. Several grading descriptors (*e.g.,* d_{50}, c_u) used in engineering practice are considered but only fines content is presented in this paper because it was found to be related to parameters that quantify engineering behaviour (*e.g.,* strength) of decomposed volcanic rocks (Okewale and Coop 2017, 2018). Relating these stiffness parameters with plasticity (Fig. 9(a) to 9(b)), samples with high plasticities typically have a lower A and higher n values, and the relationships are represented by regression lines. Therefore, plasticity might be a controlling parameter which is similar to what was observed by Vaggiani and Atkinson (1995) for clays. Figure 10 presents the relationship between the parameters and fines content. Also, the samples with high fines content have a lower A and higher n values and the trend similar to plasticity are seen. Again, this indicates that fines content might also be a controlling parameter for the decomposed volcanics.

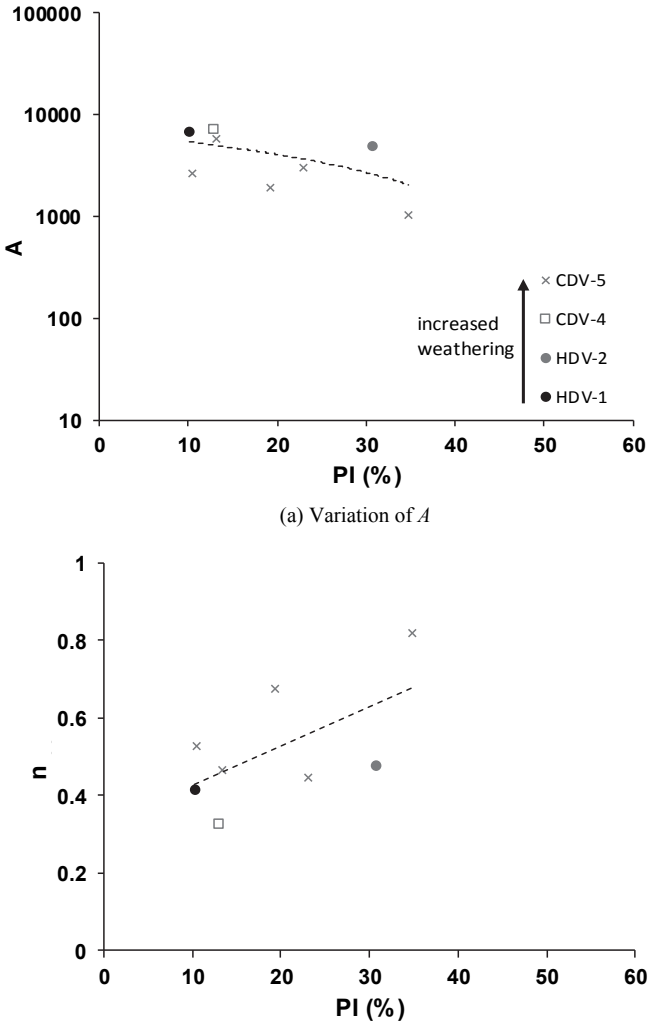

(a) Variation of A

(b) Variation of n

Fig. 9 Variation of parameters with Plasticity

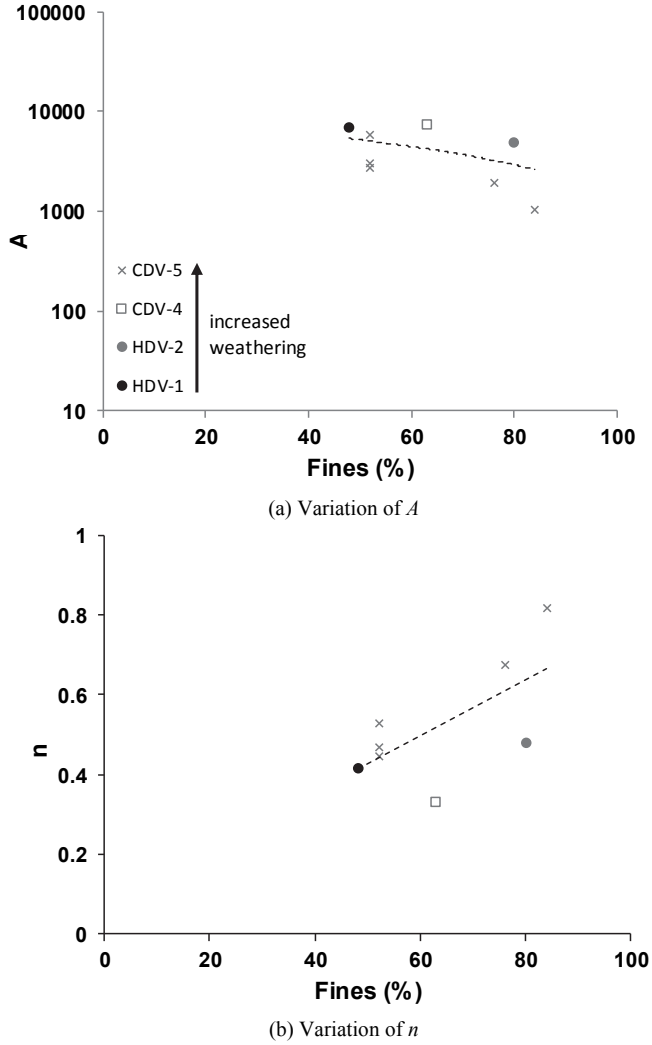

(a) Variation of A

(b) Variation of n

Fig. 10 Variation of parameters with fines content

The variation of elastic material parameters A and n with depth is presented in Fig. 11. This is very important from the geology and engineering points of view. The trends are represented by estimated trend line for parameter A and regression line for parameter n. Empty black symbols are used for the intact samples while empty grey and filled symbols are used for the reconstituted samples. Apart from the scattered data at shallow depth caused by the HDV samples and possibly as a result of heterogeneity, the A values reduce and n values increase with weathering (Figs. 11(a) to 11(b)).

3.5 Stiffness Anisotropy

Both vertically and horizontally orientated bender elements were also used, measuring the moduli in vertical plane (G_{vh}) and horizontal plane (G_{hh}) and the results for the intact and reconstituted samples are presented in Fig. 12. Grey symbols and lines are used for the G_{vh} while black symbols and lines are used for the G_{hh}. The intact sample plots above the reconstituted samples but the modulus does not increase with mean effective stress, showing effect of structure. The curves for the moduli in the vertical and horizontal planes are nearly coincident for the intact and reconstituted samples, showing no significant anisotropy in the samples.

Comparing the degree of stiffness anisotropy of CDT studied by Ng and Leung (2007), the anisotropy in the sample is low possibly because the sample was retrieved at shallow depth and small effect of structure. Also, the degree of anisotropy (taken as the ratio of G_{hh} to G_{hv}) found for other soils as presented in Table 6 in the intact and reconstituted states are higher (*e.g.,* Jamiolkowski *et al.* 1995; Pennington *et al.* 1997). This can be attributed to the nature of their formations. Generally, strong anisotropy in sample indicates higher modulus in horizonal plane (G_{hh}) which reflects stronger structure (bonding and fabric) in this plane. Clays are formed by depositional and post-depositional processes which generally increase the stiffness of reconstituted and intact samples, while the decomposed rocks are formed by disintegration of parent rocks which affects the structure as well as behavior resulting from constituent particles thereby reducing the stiffness.

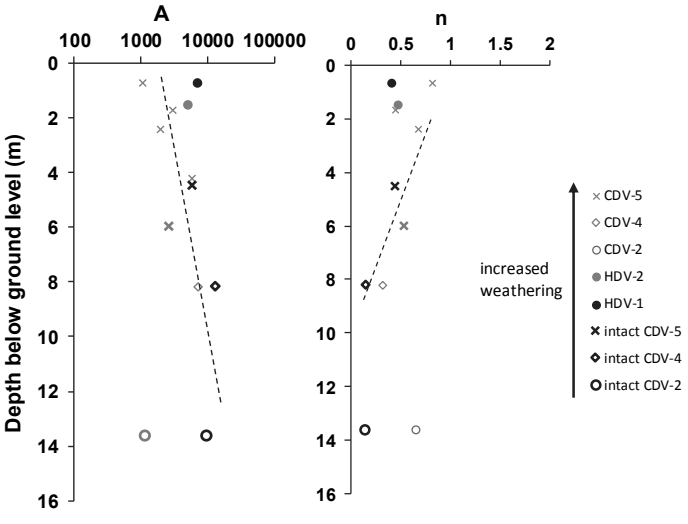

(a) Variation of A (b) Variation of n

Note: Empty black symbols for intact samples;
Grey and filled symbols for reconstituted samples

Fig. 11 Variations of material parameters with depth

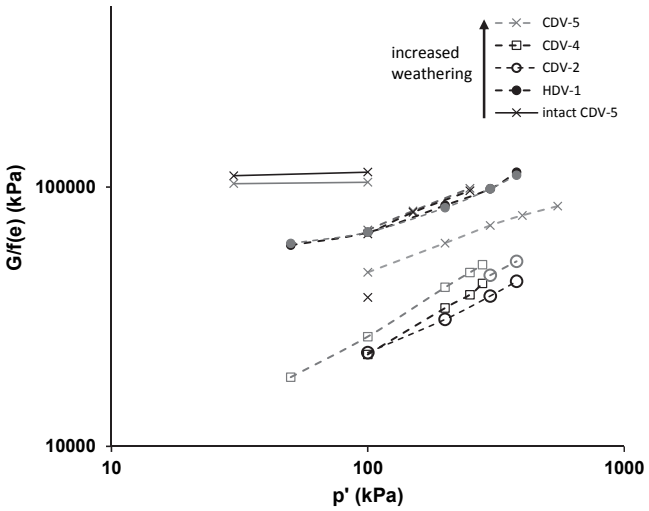

Note: Grey markers and lines are for G_{hv};
Black markers and lines are for G_{hh}

Fig. 12 Variation of normalized shear moduli in vertical and horizontal plane with mean effective stress

Table 6 Comparison of stiffness anisotropy for different geomaterials

Sample	State	G_{hh}/G_{hv}	Author(s)
Pisa clay	Intact	1.4	Jamiolkowski *et al.* (1995)
Panigaglia clay	Intact	1.6	Jamiolkowski *et al.* (1995)
Gault clay	Reconstituted	1.5	Pennington *et al.* (1997)
London clay	Reconstituted	1.24	Jovicic and Coop (1998)
London clay	Intact	1.5	Jovicic and Coop (1998)
CDT CDT	Intact (block) Intact (mazier)	1.48 1.36	Ng and Leung (2007) Ng and Leung (2007)
CDV	Reconstituted	0.95	This study
HDV	Reconstituted	0.98	This study
CDV	Intact	1.08	This study

Note: CDT completely decomposed tuff

4. CONCLUSIONS

Based on the combination of bender elements and local instrumentation measurements, the shear stiffness characteristics and the small strain behaviour of highly and completely decomposed volcanic rocks of various degrees of weathering from different locations, depths and three different formations have been investigated in the intact and reconstituted states. The extreme heterogeneity of the samples, the variability of degree of weathering as well as differences in parent rocks cause significant scatter in the data. The effects of heterogeneity are much more pronounced at small strains than large strains, resulting in less clear trend of degrees of weathering with the stiffness of the samples.

There is a non-linear relationship between modulus and shear strain, similar to other geomaterials and the curves degrade faster for the reconstituted samples than the intact samples. There are small effects of structure using lateral bender elements and local instrumentations at small strain. The modulus obtained for the intact sample using lateral bender elements is slightly higher than those of the reconstituted samples, indicating a small effect

of structure. There is also possible effect of structure at small strains.

The stiffness of the intact samples is greater than those of the reconstituted samples and it reduces with weathering. The values of elastic material parameter A are increasing with depth thereby reducing with weathering and n values are reducing with depth thereby increasing with weathering. Generally, the samples with high plasticity and fines content typically have a lower stiffness values indicating the effects of plasticity and fines content on the stiffness of the samples. The degree of anisotropy is insignificant for both the intact and reconstituted samples using lateral bender elements.

ACKNOWLEDGEMENTS

This research was fully supported by a grant from the Research Grant Council (RGC) of the Hong Kong Special Administrative Region (HKSAR), China (T22-603/15N). The author also thanks the RGC for the award of scholarship for his Ph.D study.

NOTATIONS

A	Elastic material stiffness parameter
CF	Clay fraction (%)
e	Void ratio
E_t	Tangent Young's modulus (MPa)
$f(e)$	Void ratio function
G	Shear modulus (MPa)
G_{hh}	Shear modulus in h-h plane (kPa)
G_{hv}	Shear modulus in h-v plane (kPa)
G_{vh}	Shear modulus in v-h plane (kPa)
G_{tan}	Tangent shear modulus (MPa)
G_o	Elastic shear modulus (kPa)
LL	Liquid limit (%)
M	Strength parameter
n	Elastic material stiffness parameter
PI	Plasticity index (%)
PL	Plastic limit (%)
p_r	Normalising pressure taken as 1 kPa (kPa)
p'	Mean effective stress (kPa)
p_c'	Mean effective stress after consolidation (kPa)
t_a	Shear wave arrival time (s)
v	In-situ specific volume
v_s	Velocity of travelling wave (m/s)
$v_{s(hh)}$	Horizontally transmitted shear wave velocity with horizontal polarisation (m/s)
$v_{s(hv)}$	Horizontally transmitted shear wave velocity with vertical polarization (m/s)
$v_{s(vh)}$	Vertically transmitted shear wave velocity with horizontal polarization (m/s)
ρ	Bulk density of the soil (g/cm^3)
ε_s	Shear strain (%)

REFERENCES

BS 1377:2:1990 (1990). *Methods of Test for Soils for Civil Engineering Purposes*. British Standard Institution, London.

Clayton, C.R., Theron, M., and Best, A.I. (2004). "The measurement of shear wave velocity using side-mounted bender elements in the triaxial apparatus." *Géotechnique*, **54**(7), 495-498. https://doi.org/10.1680/geot.2004.54.7.495

Cuccovillo, T. and Coop, M.R. (1997). "The measurement of local axial strains in triaxial tests using LVDT's." *Géotechnique,* **47**(1), 167-171. https://doi.org/10.1680/geot.1997.47.1.167

Gasparre, A. and Coop, M.R. (2006). "Techniques for performing small-strain probes in the triaxial apparatus." *Géotechnique*, **56**(7), 491-495. https://doi.org/10.1680/geot.2006.56.7.491

Gasparre, A., Hight, D.W., Coop, M. R., and Jardine, R. J. (2014). "The laboratory measurement and interpretation of small strain stiffness in stiff clay." *Géotechnique*, **57**(12), 942-953. https://doi.org/10.1680/geot.13.P.227

Gasparre, A., Nishimura, S., Minh, N.A., Coop, M.R., and Jardine, R.J. (2007). "The stiffness of natural London clay." *Géotechnique*, **57**(1), 33-47. https://doi.org/10.1680/geot.2007.57.1.33

Geotechnical Engineering Office. (1988). *Guide to Rock and Soil Descriptions*, *Geoguide 3*. Geotechnical Engineering Office, Civil Engineering Department, Government of the Hong Kong SAR.

Hardin, B.O. and Drnevich, V.P. (1972). "Shear modulus and damping in soils: Measurements and parameter effects." *Journal of the Soil Mechanics and Foundations Division*, ASCE, **98**(6), 603-624.

Hardin, B.O. and Richart, F.E. (1963). "Elastic wave velocities in granular soils." *Journal of the Soil Mechanics and Foundations Division*, ASCE, **89**(1), 33-65.

ISRM (2007). *The Complete ISRM Suggested Methods for Rock Characterization, Testing and Monitoring [1974–2006]*. Ulusay, R., Hudson, J., Eds., International Society of Rock Mechanics.

Irfan, T.Y. (1996). *Mineralogy and Fabric Characterization and Classification of Weathered Granitic Rocks in Hong Kong,* Geotechnical Engineering Office, Report No.41, Geotechnical Engineering Office, Hong Kong.

Jamiolkowski, M., Lancellotta, R., and Lo Presti, D.C.F. (1995). "Remarks on the stiffness at small strains of six Italian clays." *Proceedings of International Symposium on Prefailure Deformation of Geomaterials*, Torino, 817-836.

Jovičić, V. and Coop, M.R. (1997). "Stiffness of coarse-grained soils at small strain." *Géotechnique*, **47**(3), 545-561. https://doi.org/10.1680/geot.1997.47.3.545

Jovičić, V. and Coop, M.R. (1998). "The measurement of stiffness anisotropy in clays with bender element tests in the triaxial apparatus." *Geotechnical Testing Journal*, ASTM International, **21**(1), 3-10. GTJ10419J.

Lo Presti, D.C.F. (1995). "General report: Measurement of shear deformation of geomaterials in the laboratory." *Proceedings of International Symposium on Prefailure Deformation of Geomaterials*, Torino, 1067-1088.

Ng, C.W.W. and Leung, E.H.Y. (2007). "Determination of shear wave velocities and shear moduli of completely decomposed tuff." *Journal of Geotechnical and Geoenvironmental Engineering*, ASCE, **133**(6), 630-640. http://doi.org/10.1061/(ASCE)1090-0241(2007)133:6(630)

Ng, C.W.W., Leung, E.H.Y., and Lau, C.K. (2004). "Inherent anisotropic stiffness of weathered geomaterial and its influence on ground deformations around deep excavations." *Canadian Geotechnical Journal*, **41**(1), 12-24. http://doi.org/10.1139/T03-066

Ng, C.W.W., Pun, W.K., and Pang, R.P.L. (2000). "Small strain stiffness of natural granitic saprolite in Hong Kong." *Journal of Geotechnical and Geoenvironmental Engineering*, ASCE, **126**(9), 819-833. https://doi.org/10.1061/(ASCE)1090-0241(2000)126:9(819

Ng, C.W.W. and Wang, Y. (2001). "Field and laboratory measure-

ment of small strain stiffness of decomposed granites." *Soils and Foundations,* **41**(3), 57-71.

Okewale, I.A. (2019). "Influence of fines on the compression behaviour of decomposed volcanic rocks." *International Journal of Geo-Engineering*, **10**(4), 1-17. https://doi.org/10.1186/s40703-019-0101-y

Okewale, I.A. and Coop, M.R. (2017). "A study of the effects of weathering on soils derived from decomposed volcanic rocks." *Engineering Geology*, **222**, 53-71. http://dx.doi.org/10.1016/j.enggeo.2017.03.014

Okewale, I.A. and Coop, M.R. (2018). "Suitability of different approaches to analyze and predict the behaviour of decomposed volcanic rocks." *Journal of Geotechnical and Geoenvironmental Engineering*, ASCE, **144**(9), 1-14. http://doi.org/10.1061/(ASCE)GT.1943-5606.0001944

Pennington, D.S., Nash, D.F.T., and Lings M.L. (1997). "Anisotropy of G_o shear stiffness in Gault clay." *Géotechnique*, **47**(3), 391-398.

Rocchi, I. and Coop, M.R. (2015). "The effects of weathering on the physical and mechanical properties of a granitic saprolite." *Géotechnique*, **65**(6), 482-493. https://doi.org/10.1680/geot.14.P.177

Shibuya, S., Hwang, S.C., and Mitachi, T. (1997). "Elastic shear modulis of soft clays from shear-wave velocity measurement." *Géotechnique*, **47**(3), 593-601. https://doi.org/10.1680/geot.1997.47.3.593

Vaggiani, G. and Atkinson, J.H. (1995). "Stiffness of fine-grained soil at very small strains." *Géotechnique*, **45**(2), 249-265. https://doi.org/10.1680/geot.1995.45.2.249

Viana Da Fonseca, A., Matos Fernandes, M., and Silva Cardoso, A. (1997). "Interpretation of a footing load test on a saprolitic soil from granite." *Géotechnique*, **47**(3), 633-651. https://doi.org/10.1680/geot.1997.47.3.633

Wang, Y. and Ng, C.W.W. (2005). "Effects of stress paths on the small-strain stiffness of completely decomposed granite." *Canadian Geotechnical Journal*, **42**, 1200-1211. http://doi.org/10.1139/T05-009

Wroth, C.P. and Houlsby, G.T. (1985). "Soil mechanics, property characterisation and analysis procedure." *Proceedings of XI ICSMFE*, San Francisco, 1-55.